CHAPTER 5

DEVELOPMENT OF SILVER NANOPARTICLES

5. Development of silver nanoparticles

5.1 Experimental works

5.1.1 Materials

Silver nitrate was procured from Himedia laboaratories pvt. Ltd. (Mumbai, India), Bovine albumin was obtained from SD Fine Chemical Ltd. (Mumbai, India), standard campesterol was procured from KV Bioscientific (Lucknow, India) while quercetin, rutin and lupeol was procured from Himedia laboaratories pvt. Ltd. (Mumbai, India). All the other chemicals and solvents were of AR grade. Double distilled water was utilised throughout the experimental work.

5.1.2 Extract preparation and fractionation

The leaves of *Blumea lacera* plant were collected from the local areas of Varanasi, U.P., dried and crushed into powder and then 100g of crushed powder was weighed. This was then subjected for hydroalcoholic maceration (solute: solvent ratio; 1:3) for three consecutive days and the material was filtered after every day without pressing the marc except last day. After the extraction was complete the material was finally filtered and marc was pressed. Thereafter, all the filtrate obtained were mixed and concentrated in rotary evaporator (IKA, Germany) at 70°C and 65 RPM. The concentrated and dried extract (EBL) was fractionated through successive solvent fractionation technique using different solvents in increasing order of polarity. By using this technique, five different fractions *viz*. hexane fraction (HF), ethyl acetate fraction (EAF), dichloromethane fraction (DCMF), butanol fraction (BuOHF) and aqueous fraction (AF) were prepared and stored until further analysis such as preformulation studies **(figure 5.1)**.

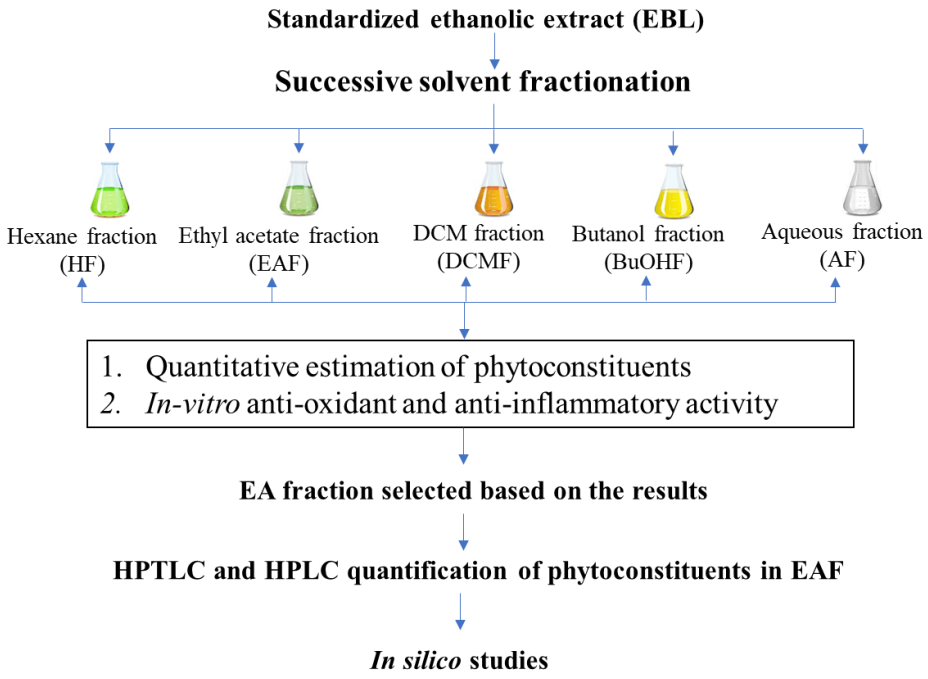

Figure 5. 1: Graphical representation of preformulation studies.

5.1.3 Quantitative phytochemical estimation

It included estimation of total phenolic, total flavonoid, total flavonol and total phytosterol content in the fractions obtained by successive solvent fractionation of EBL.

5.1.3.1 Determination of total phenolic content

The estimation of total phenolic content was carried out by folin coicalteau calorimetric method as by Hagerman A, et al., 2000 [126] with some modifications. Gallic acid (500mg) was weighed accurately and dissolved in 10ml ethanol, and then the volume was made up to 100ml with triple distilled water (TDW). Sodium carbonate (20g) was weighed accurately and dissolved in 80ml of TDW. It was then subjected to heating on water bath till boiling, then cooled and finally the volume was made up to 100ml with TDW. For the preparation of standard curve different concentrations 0, 1, 2, 3, 4, 5 and 10ml of the gallic acid stock solution

was transferred to series of the 100ml volumetric flask and the volume was made up to mark. Then 1ml was transferred from each of the volumetric flasks in each separated test tubes. 8ml of TDW and 0.5ml of 2N Folin-ciocalteau reagent (FCR) was added to each of the test tube followed by vigorous mixing. After 5 min. 1.5 ml of 20% sodium carbonate stock solution was then added to each of the test tube followed by proper mixing. Finally, the whole prepared solution was kept for 2hr after which the absorbance was taken using UV-Visible spectrophotometer (Shimadzu pharmaspec-1700). Fractions (100mg) from EBL were weighed accurately and dissolved in 100ml of TDW to make the stock solution. One ml of this stock solution was transferred to a test tube and 8ml of TDW was again added followed by 0.5ml of FC reagent and 1.5ml of Na_2CO_3 solution. In addition, blank solution was also prepared in the same way without the crude drug. Absorbance was recorded at 765nm against blank using UV-Visible spectrophotometer and the total phenolic contents were expressed in terms of gallic acid equivalent (mg/g of dry mass).

5.1.3.2 Estimation of total flavonoid

The determination of the total flavonoid content was carried out based on the aluminum chloride method using rutin as the standard reference compound [29]. The method was based on the formation of a flavonoid-aluminium complex having the absorptivity maximum at 415nm. Standard rutin solution (0.5mg/ml) was prepared 5mg of rutin in 10ml pure methanol which is equivalent to 0.5mg/ml. Twenty percent aluminum chloride was prepared by dissolving 20gm of anhydrous aluminum chloride in 100ml methanol. Fractions (100µl) in methanol (10mg/ml) was mixed with 10µl of 20% aluminum trichloride in methanol and a drop of acetic acid, and then diluted to 5 ml. The absorption at 415nm was read after 40min.

blank samples were prepared by 100µl of plant extracts and a drop of acetic acid and then diluted to 5ml with methanol. The absorption of standard rutin solution (0.5mg/ml) in methanol was measured under the same conditions.

5.1.3.3 Estimation of total flavonol content

The method was done as per the procedure proposed by [29]. Standard rutin solution (0.5 mg/ml) was prepared by dissolving 5mg of rutin in 10ml pure methanol which is equivalent to 0.5mg/ml. One gram of aluminum chloride was accurately weighed and dissolved in 50ml volume methanol; this is equivalent to 20mg/ml aluminum chloride. Accurately weighed 2.5gm of sodium acetate was dissolved in 50ml of methanol which is equivalent to 50mg/ml of sodium acetate. One ml of fraction (10mg/ml) was mixed with 1 ml aluminum trichloride (20mg/ml) and 3ml sodium acetate (50mg/ml). The absorbance at 440nm was read after 2.5hr. The absorption of standard rutin solution (0.5mg/ml) in methanol was measured under the same conditions.

5.1.3.4 Estimation of total phytosterol content

Total phytosterol content, determined as per the method described by Araújo. *et al.* [127]. Briefly, Hydroethanolic extract (100 ml) was dried under reduced pressure at 40°C. The residue was resuspended in 20 ml of chloroform and the volume adjusted to 50 ml with the same solvent (SM). SM aliquots were transferred to 10 ml volumetric flasks and 2 ml of LB reagent was added. The volume was adjusted with chloroform. The absorptions were measured in a spectrophotometer UV/Vis (Evolution 60S, Thermo Scientific®, Germany), 5 min after the addition of the reagent LB. The chloroform was used as a blank. Aliquots of the samples were analyzed in a scanning spectrophotometer in the region 400-900 nm, 5 min after addition

of the reagent, and the chloroform measured using the blank. The spectra were used to identify the most appropriate dilutions and determine the wavelength of maximum absorption. The influence of the reaction time on the responses of the method is both the samples and for the standard (β-sitosterol) was studied by performing a kinetic reaction. For this purpose, after addition of the reagent, the absorbance was measured every 5 min for 1 h. The samples were prepared as described above, and transferred to 10 ml volumetric flasks. Different aliquots of reagent LB (1, 2 and 3 ml) were added and the volume was adjusted with chloroform. After 5 min, the absorbances were measured in the UV-Visible spectrophotometer, using chloroform to the blank. The phytosterol content (TPC) was calculated as β-sitosterol (g%) using the photometric standard equation to calculate steroids (Eq. 5.1).

$$TPC = \mathrm{Cs}\frac{\mathrm{Aa}}{\mathrm{As}} \times 100 \qquad (\mathrm{Eq.}\ 5.1)$$

Where: Cs= Standard Concentration; Aa = Absorbance of the sample; As =Absorbance of the standard.

5.1.4 *In vitro* antioxidant activity

The study dealt with total antioxidant capacity, DPPH radical scavenging activity, alkaline dimethyl sulfoxide (DSMO) method for scavenging of the superoxide radical and the hydrogen peroxide scavenging activity.

5.1.4.1 Total antioxidant assay

Phosphomolybdenum method described by Prieto et al. [128] was followed to assess the total antioxidant capacity of all five fractions from EBL and PLSNPs. Briefly, 0.3 ml of EAF/PLSNPs in methanol (1 mg/ml) and ascorbic acid (50-300 µg/ml) were mixed separately with 3 ml of study reagent (0.6 M H_2SO_4, 28 mM Na_3PO_4 and 4 mM $(NH_4)_6Mo_7O_{24}$). All the

tubes were sealed and incubated in a boiling water bath at 95ºC for 90 min. After cooling to room temperature, the absorbance of each sample was measured at 695 nm against the blank (3 ml of reagent solution+0.3 ml methanol). The total antioxidant capacity was expressed as the number of equivalents of ascorbic acid.

5.1.4.2 DPPH free radical scavenging activity

The free radical scavenging capacity of fractions/PLSNPs was assessed by the 1, 1-diphenyl-2-picryl-hydrazil (DPPH) method [129]. In brief, 5 ml of DPPH solution (100 µM/ml in methanol) was added to 1ml of sample in different concentrations (25–200 µg/ml). The absorbance was than measured after 30 min at 517 nm. The free radical scavenging activity was calculated using the following equation:

$$DPPH\ scavenging\ effect = 1 - \frac{A_1}{A_0} \times 100 \quad \text{(Eq 5.2)}$$

Where, A_0 is the absorbance of the blank and A_1 is the absorbance of test solution. Further, percent inhibition was plotted and IC_{50} was calculated with respect to ascorbic acid (positive control).

5.1.4.3 Scavenging of hydrogen peroxide

Scavenging capacity of fractions/PLSNPs was determined using the method by Jayaprakasha et.al. [130]. A 20 mM solution of hydrogen peroxide (H_2O_2) was prepared in phosphate buffered saline (PBS, pH 7.4). Then, 1 ml fractions/PLSNPs in varying concentrations and standards in methanol were added to 2 ml of above H_2O_2 solution. At last, after 10 min incubation, the absorbance was recorded at 230 nm. All readings were recorded in triplicates and then the calculation for percentage inhibition was done.

5.1.4.4 Assay for reducing power

Assay for reducing power was carried out by potassium ferricyanide method [131]. Briefly, 1 ml of fractions/PLSNPs (final concentration 25-200 µg/ml) were admixed with 2.5 ml PBS (0.2M, pH 6.6) and 2.5 ml $K_3Fe(CN)_6$ (10 g/L). The resulting mixture was then incubated for 20 minutes at 50℃. To this, 2.5 ml of trichloroacetic acid (100 g/L) was incorporated, then centrifuged for 10 min at 300 rpm. Finally, the supernatant solution (2.5 ml) was collected followed by mixing with DW (2.5 ml) and 0.5 ml of $FeCl_3$ (1 g/L) and absorbance was recorded at 700 nm. Ascorbic acid served as positive control and PBS as a blank solution.

5.1.4.5 Nitric oxide scavenging assay

Nitric oxide scavenging assay was done using sodium nitroprusside [132]. In brief, 2 ml (10 mM) sodium nitroprusside in 0.5 ml PBS (pH 7.4) was admixed with varying concentrations of fractions/PLSNPs (0.5 ml) and the mixture was then incubated at 25°C for about two and a half hours. Aliquot of 0.5 ml was taken out from the above mixture and added to 1 ml of sulfanilic acid (SA) reagent (33% SA in 20% glacial acetic acid) and again incubated at 25°C for 5 min. Finally, 1 ml naphthyl ethylenediamine dihydrochloride (0.1% w/v) was added and left for 30 min at 25°C. At last, the absorbance was recorded at 546 nm. The nitric oxide radical scavenging activity was calculated and percentage inhibition and IC_{50} was calculated using rutin, as positive control.

5.1.4.6 Scavenging of hydroxyl radical by deoxyribose method

Hydroxyl radical scavenging capacity of fractions/PLSNPs was determined by assessing degradation of Deoxyribose [133]. The final reaction mixture (1.2 ml) contained the aliquots (0.2 ml) of varying concentrations of the fractions/PLSNPs, ferric chloride (0.1 mM, 0.2 ml),

EDTA (0.1 mM, 0.2 ml), ascorbic acid (0.1 mM, 0.2 ml) and H_2O_2 (2 mM, 0.2 ml) in PBS (pH, 7.4, 20 mM). These mixtures were then incubated at 37°C for 30 min. Thereafter, 0.2 ml of ice-cold trichloro acetic acid (15%, w/v) and 0.2 ml thiobarbituric acid (1% w/v in 0.25 N HCl) were added to the reaction mixtures and kept in a boiling water bath. After 30 minutes, the reaction mixtures were taken off and the absorbance was measured at 532 nm when the reaction mixture was cool. All the absorbance were recorded in triplicates and the percentage inhibition was calculated using equation (Eq 5.2).

5.1.5 *In vitro* anti-inflammatory activity

With slight modifications, the *in vitro* anti-inflammatory potential of EAF and PLSNPs was determined as per previous reports by assessing the inhibition of protein (albumin) denaturation and antiproteinase activity [134, 135]. EAF and PLSNPs were serially diluted in deionised water (DW) from 200 to 1200 µg/ml for protein denaturation and 100 to 1000 µg/ml respectively. Aspirin (100 µg/ ml, Sigma-Aldrich, Singapore), a standard anti-inflammatory drug, was used as a positive control, whereas DW was used as a negative control.

5.1.5.1 Inhibition of albumin denaturation

The reaction mixture, containing 1ml of one percent solution of bovine albumin fraction in water was added into 1 ml of EAF/PLSNPs solution. This reaction mixture was incubated for 20 min at 37°C followed by heating to 51°C for 30 min after adjusting the pH 6.3. Thereafter, the reaction mixture was allowed to cool to room temperature, then absorbance was measured at 660 nm (Agilent UV-Visible Spectrophotometer). The following equation was used for calculating percentage inhibition of protein denaturation, and the concentration required for a 50% inhibition was expressed as IC_{50} values:

$$Percentage\ inhibition\ (\%) = \frac{A_{Control} - A_{Sample}}{A_{Control}} \times 100 \qquad \text{Eq. (5.3)}$$

Where, $A_{control}$ is the absorbance of DW and A_{sample} is the absorbance of the EAF/PLSNPs.

5.1.5.2 Antiproteinase activity

The reaction mixture was prepared by adding 0.06 mg trypsin followed by 1mL of EAF/PLSNPs into 1 mL of 20 mM Tris HCl buffer (pH 7.4) and incubated at 37°C for 5 min. To this, 1 mL of 0.8% (w/v) casein was then added and further incubated for 20 min. At last, the reaction was terminated by adding 2 mL perchloric acid (70%) and the mixture was centrifuged at 4°C, 6,000 rpm, for 10 min. The supernatant was collected, and absorbance was measured at 210 nm (Agilent UV-Visible Spectrophotometer). The percent proteinase inhibition was calculated using the equation given below, and the results were expressed as IC_{50} values:

$$Percentage\ inhibition\ (\%) = \frac{A_{Control} - A_{Sample}}{A_{Control}} \times 100 \qquad \text{Eq (5.4)}$$

5.1.6 Standardization of fractions from EBL and quantification of phytoconstituents by HPTLC

The marker-based standardization was carried out to standardize EBL and its fractions with respect to campesterol by High Performance Thin Layer Chromatography (HPTLC)-based densitometric method. Different volumes (2 to 8 µl) of standard solutions (0.05 mg/ml) and sample solution (2 and 5 µL in methanol), were applied as a band on HPTLC silica gel $60F_{254}$ aluminium plates (20×10 cm). The bands (8 mm wide) were applied at 8 mm on Y-axis and 20 mm on X-axis of the HPTLC plate by Linomat applicator (CAMAG Scientific,

Switzerland). The plates were then kept for development in the pre-saturated (20 min) twin-trough chamber. using. The mobile phase used was hexane: chloroform: ethyl acetate (in a ratio 7:2:1 v/v) as mobile phase. The solvent front position was 70 mm at 25±2 °C and RH 40%. The plates were dried on a TLC plate heater (CAMAG Scientific, Switzerland) at 60°C for 5 min after development. The plates were then dipped in derivatizing chamber filled with freshly prepared p-anisaldehyde–sulfuric acid (derivatizing reagent). After dipping, the plates were again dried on a TLC plate heater at 110°C for 10 min. After derivatization, different coloured bands appeared indicating the marker compounds. These bands were then scanned at different wavelengths using TLC Scanner 4 (CAMAG Scientific, Switzerland). The amount of campesterol present in samples was quantified using linear regression equation with the help of Vision CATS software by CAMAG Scientific, Switzerland.

5.1.7 Standardization of EAF by HPLC

To confirm the presence of campesterol in EAF and PLSNPs, the retention time and UV spectra of sample and standard campesterol was done using Waters 1500-series pump (Milford, MA, USA) attached to Waters 2998 photodiode array detector. The mobile phase and samples were filtered through a membrane filter (0.45 µm) using solvent filtration apparatus (Millipore, USA) and de-aerated prior to use. The chromatographic conditions were as follows: the column used was Lichro CART® 250-4 C18 column, and the mobile phase, methanol-water (95:05 v/v) were used in isocratic flow (1.0 ml/min) for sharp peak shape and resolution at wavelength UV 210 nm. The injection volume was 15 µl, and all chromatographic operation was conducted at room temperature. Quantification of campesterol in EAF was done in waters Breeze software (Waters, USA) using linear equation- $y = 52356x + 3000000$.

5.1.8 Molecular docking studies on endothelin 1, AMPK and cytokines (TNFα and IL-6)

The crystal structure of Endothelin 1 complexed with K-8794 (PDB ID: 5X93) [136] AMPK (PDB ID: 4CFF) [137] and IL-6 (PDB ID: 1ALU) [138] and TNF-α (PDB ID: 2AZ5) [139] was downloaded from the protein data bank (PDB) site (https://www.rcsb.org/) [140]. Preparation of protein structures, discovery Studio 2021 client version [141] was used. Energy minimization of protein was done using an Amber module that includes, NMR refinement, molecular dynamics, and energy minimization. The 2D structure of ligands was drawn on Chem 3D 20.1.1 software and ligand energies were minimized to optimize the bond length and bond angle. After completion of above sequential steps, Auto dock 4 software [142] was used for docking studies.

5.1.9 Synthesis of silver nanoparticles (PLSNPs)

After preliminary process optimization [143], 680 mg of silver nitrate was dissolved in 800 ml of deionised water in a 1 litre flask. To this, 200 ml of EAF (0.1 mg/ml in water) was added and adjusted the pH to 6.5. The mixture was incubated at 60°C for 3 hours followed by overnight reaction at room temperature. The effective synthesis of PLSNPs was verified from the change in colour from pale yellow to reddish brown colour. The biosynthesized PLSNPs were purified by centrifuging at 10,000 rpm for 20 minutes. Supernatant was discarded, the remaining ions and impurities from the PLSNPs were separated by resuspending in deionized water and again centrifuging at 10,000 rpm for 10 minutes. The pelleted PLSNPs was transferred onto a previously weighed glass petri plate and freeze dried in lyophilizer (FreeZone 1, Labconco, USA). After the removal of water, dried PLSNPs were weighed and stored until further analysis.

5.1.10 Process optimization

Design Expert (Version 12.0.0 Trial, Stat-Ease Ink.) was used to determine the boundary of the experiment, for evaluating response and for finally optimizing the process. The level of design factors has been represented in **Table 5.1**.

Table 5. 1- Input factors with their ascribed values and coded levels, along with the expected outcomes of the response.

Factor	Levels used, Actual (coded)		
	Low (-1)	Medium (0)	High (+1)
X_1= EAF conc. (mg/ml)	1	2	3
X_2=$AgNO_3$ conc. (mM)	2	4	6
X_3=Time (h)	12	24	36
Dependent Variables	Constraints		
Y1= Particle size (nm)	In range		
Y2= Entrapment Efficiency (%)	Maximize		

The actual extractive experiments with values of independent variables and obtained results are shown in **Table 5.2**. A total of 20 experiments were performed. The particle size was measured using particle size analyzer while entrapment efficiency was estimated via standard method. The particle size of 20 models was calculated after their extraction process. These extraction test models were put for time period obtained after input of independent variables. Repetition of models are recommended to obtain proper error of the model. These actual runs are compared with predicted values of the software. The values of mean, median, variance was calculated in the software which helps in integral analysis of the experiments. It also goes through the process of evaluating standard error, standard mean error which are important for knowing the spread ability of the model.

Table 5. 2- Actual extractive runs for obtainment of best results (mean±SEM)

Batch	Independent variables			Dependent variables	
	A: EAF conc. (mg/mL)	B: $AgNO_3$ conc. (mM)	C: (Time; h)	Y_1: Particle size (nm)	Y_2: Entrapment efficiency (%)
1	1	4	36	96.4±3.48	45.47±5.09
2	1	4	12	40.63±6.27	38.64±3.48
3	3	4	36	128.09±4.62	99.7±7.47
4	2	4	24	86.21±3.13	86.85±2.95
5	2	4	24	89.37±7.32	92.03±2.54
6	3	6	24	58.72±4.83	63.48±4.27
7	2	4	24	63.81±5.66	84.91±3.69
8	1	6	24	71.49±2.98	35.38±5.82
9	3	4	12	96.44±4.37	51.39±3.67
10	2	2	12	40.38±7.04	58.35±6.85
11	1	2	24	60.19±2.55	35.67±7.32
12	2	2	36	96.35±3.13	72.41±2.86
13	2	6	12	45.23±5.23	54.66±3.58
14	2	4	24	91.34±3.47	87.62±5.74
15	3	2	24	121.32±2.82	89.02±7.38
16	2	4	24	89.48±4.72	93.11±3.57
17	2	4	24	83.71±3.56	84.72±4.60
18	2	4	24	86.57±6.25	91.57±2.63
19	2	6	36	39.64±5.64	98.01±3.10
20	2	4	24	92.55±2.55	56.73±6.54

5.1.11 Check point analysis (validation of method)

By creating a checkpoint batch (n = 3) of an optimised formula in ideal conditions as advised by Design-Expert software and analysing the corresponding CQAs, the predictability/validity of the rotatable BBD model was confirmed (saturation solubility). By calculating the

percentage prediction error (percent Bias) using Eq. (5.5), a quantitative comparison between the theoretical predictions made using software and the actual experimental data was made [116].

$$\text{prediction error (\%)} = \frac{\text{experimental value} - \text{predicted value}}{\text{predicted value}} \times 100 \qquad \text{Eq(5.5)}$$

5.1.12 Characterization of PLSNPs

5.1.12.1 UV-Visible spectrophotometric analysis

The green synthesized PLSNPs colloidal solution was characterized using UV-Visible spectrophotometer (Shimadzu, Japan) over the wavelength range of 200-600nm using deionized water as blank. The absorption spectrum and maximum absorption wavelength were recorded for PLSNPs and $AgNO_3$ solution.

5.1.12.2 Attenuated Total Reflectance-Fourier Transform Infrared spectroscopy (ATR-FTIR analysis)

The ATR-FTIR was performed to identify the functional groups present in phytochemicals responsible for the synthesis as well as capping and stabilizing the synthesized PLSNPs. PLSNPs and EAF were spread uniformly on ATR crystal and the molecular vibrational spectra were recorded over the wavelength of $4000cm^{-1}$-$400cm^{-1}$.

5.1.12.3 Morphological analysis

Morphological analysis of PLSNPs was carried out by TEM, SEM. The hydrodynamic particle size (Zavg), size distribution, and polydispersity index (PDI) of PLSNPs were examined by particle size analyser (Malvern Zeta particle size analyzer, Nano ZS-90) at 25 ^{o}C. Briefly, the

PLSNPs was diluted 10 times with ultrapure water, filtered through 0.45 µm syringe filter and analyzed by particle size analyser. The morphological evalyations were carried out by TEM and SEM analysis. The size and shape of individual PLSNPs were determined by TEM (Tecnai G2 20 TWIN, FEI, USA) operated at 200 KV. Diluted PLSNPs solution (10 µl) were poured on the 3 mm diameter of carbon coated Cu grid and allowed to dry overnight at 40°C. Then the size and shape of PLSNPs were observed under TEM. The nature of synthesized particles (Crystalline or Amorphous) was determined by the Selected Area Electron Diffraction (SAED) Pattern. Three-dimensional shape of PLSNPs was examined under SEM (Carl Zeiss Microscopy Ltd., USA) operating at 20KV. Diluted solution (20 µl) of PLSNPs was spread on a clean transparent glass side and was kept in hot air oven for drying. The particles on slide were gold coated of 10nm thickness using Desk Sputter Coater machine (DSR 1, Nanostructured Coating Co., Iran). Furthermore, the morphology of PLSNPs were observed in SEM with different magnification. Then, the elemental composition of PLSNPs was determined using EDS analysis.

5.1.12.4 X-ray diffraction (XRD) analysis

The phase composition of PLSNPs was determined by X-ray diffraction (XRD) method using X-ray diffractometer (Rigaku miniflex 600, Japan). Firstly, PLSNPs solution was poured upon a silicon base followed by drying at ambient temperature. Then, the XRD diffractogram was recorded from 2θ ranging from 20 to 80° at 0.02°/minute with 2s constant time.

5.1.12.5 TGA and DSC analysis

By using the Hitachi thermal analysis equipment to perform TGA and DSC characterization, the thermal stability of synthesised PLSNPs was assessed (Hitachi, Austin, TX, USA). TGA

was utilised to research how much weight PLSNPs lost. The thermal behaviour of PLSNPs was studied using a conventional differential scanning calorimeter. After lyophilization, PLSNPs were used for TGA and DSC analyses. In order to prevent direct contact, we cleaned the alumina crucible with acetone and connected it to another crucible (reference). A nitrogen flow rate of 40 mL/min was maintained while 9.3 mg of PLSNPs were heated in the crucible at a rate of 10 °C per minute from 40 to 900 °C. Throughout the analysis, the nitrogen level was periodically monitored. Throughout the analysis, the nitrogen level was periodically monitored.

5.1.13 Estimation of entrapment efficiency (EE) and drug loading capacity (DLC)

PLSNPs (1 g) were separated from its colloidal solution by cooling centrifugation (C-24 plus, REMI, India) at 10,000 rpm and –4 ºC for 20 minutes. Separated PLSNPs were diluted up to 10 ml in methanol and sonicated for 1 hour to obtain a clear solution. The amount of campesterol entrapped was determined by spectrophotometric method at 210 nm (Agilent UV-Visible spectrophotometer). Methanol served as blank in this process. The %EE and %DLC of PLSNPs was calculated as follows:

$$\% E.E = \frac{Amount\ of\ campesterol\ (CPT)\ entrapped}{Total\ amount\ of\ campesterol} \times 100 \qquad \text{Eq (5.6)}$$

$$\% D.L.C. = \frac{Amount\ of\ CPT\ in\ the\ PLSNPs - Amount\ of CPT\ in\ the\ supernatant}{Tweight\ of\ HSNPs} \times 100 \qquad \text{Eq (5.7)}$$

5.1.14 *In vitro* release profile of PLSNPs

For *in vitro* release study, dialysis bag method was adopted, and the study was carried out in both, simulated gastric (SGF, pH 1.2) and intestinal (SIF, pH 6.8) fluids. The release pattern of campesterol from PLSNPs was determined using cellulose membrane (MWCO: 12,000–

14,000). The membranes were immerged for 12 hours in the release medium prior to use. Thereafter, PLSNPs (10 mg in 1 ml SGF or SIF) were filled in two dialysis bags respectively and hermetically sealed at both ends to avoid any leakage. Thereafter, both the dialysis bags were dipped into two separate 50 ml beakers filled with 40 ml SGF and SIF respectively. Both the beakers were placed and stirred at 100 rpm on magnetic stirrer while the temperature was kept constant (37±0.5°C) throughout the study (48 h). At specific time intervals, 5 ml sample aliquots were withdrawn and replaced by fresh buffer for maintaining sink conditions. The collected samples were analysed for campesterol content at 206 nm. To avoid any interference, blank (only SGF or SIF) was treated in the same manner.

5.1.15 Antibacterial activity

MIC of PLSNPs was determined using CLSI M07-A7 (*Nutrient Broth dilution)* method [144]. In each of the twenty test tubes (previously sterilised and dried), 5 ml of sterilised Nutrient Broth (NB) was added. In first 8 test tubes, 1 ml of different concentrations of synthesised PLSNPs suspension ranging from 10 µg/ml to 80 µg/ml were added respectively and marked as Gram +ve. The same was repeated for another 8 test tubes, marked as Gram –ve. The remaining 4 tubes were kept as blank, drug control (only PLSNPs suspension), G+ve control and G–ve control respectively. Furthermore, 1ml (10^8 CFU/ml, 0.5 McFarland's standard) of G+ve strain (*Streptococcus aureus*) was added in each G+ve tube and 1mL (10^8 CFU/ml, 0.5 McFarland's standard) G–ve strain (*Escherichia coli*) was added in each G-ve tube except blank and drug control. Finally, the equal volume (7 ml) in each tube was maintained by adding distilled water and then, incubated at 37^{o}C for 24 hours. After incubation, the MIC was measured by observing the turbidity [145, 146]. Tests for EAF and Gentamicin (standard drug) were performed in similar fashion as PLSNPs.

The antibacterial activity of PLSNPs was determined against *S. aureus* ATCC 25923 (Gram positive) and *E. coli* ATCC 25922 (Gram negative) bacterial strains by agar disk diffusion method as described by the clinical laboratory standards institute [147]. Briefly, colonies from an overnight culture of tested bacteria grown on nutrient agar were suspended in 3 ml saline and turbidity was adjusted to 0.5 McFarland ($1–2 \times 10^8$ CFU ml^{-1}) and uniformly spread with the help of sterile swab stick on MHA plates. Then, 40 µl of PLSNPs, EAF, blank and Positive control Gentamicin Disk (10 µg) was added on each culture-loaded MHA plate. All the sample loaded plates were incubated at 37ºC for 18 h. After incubation, the zone of inhibition was measured and recorded in millimeters.

5.1.15 Statistical analysis:

The experimental results are represented as mean ± SEM (n=6). The statistical analysis was carried by one-way ANOVA with Tukey's post-hoc test, using GraphPad Prism software (version: 5.03, San Diego, USA). The data considered to be statistically significant $p < 0.05$.

5.2 Results

5.2.1 Quantitative phytochemical estimation

The results of quantitative estimation of all five fractions of EBL is given in **Table 5.3**. The test results confirmed that the total phenolic (377.601± 4.00 mg/g), total flavonoids (248.564±6.77 mg/g), total flavonol (51.116± 5.76 mg/g) and total phytosterol (358.753±6.31 mg/g) content in EAF was highest among all the other fractions from EBL.

Table 5. 3- Estimation of various classes of phytoconstituents in fractions from EBL

Sample	Total phenolic content (mg/g GAE)*	Total flavonoid content (mg/g RE)*	Total flavonol content (mg/g RE)*	Total phytosterol content (mg/g BS)*
Hexane fraction (HF)	224.566± 6.19	186.371± 10.39	34.877± 5.80	262.594±16.80
Ethyl Acetate fraction (EAF)	377.601± 4.00	248.564±6.77	51.116± 5.76	358.753±6.31
Dichloromethane fraction (DCMF)	226.401± 7.57	215.625±3.34	38.495± 2.90	211.706±18.41
Butanol fraction (BuOHF)	125.202± 5.93	65.499± 9.02	17.933± 1.27	112.895±11.37

*The results are average of three determinations ± SEM

5.2.2 *In vitro* antioxidant activity of EBL fractions

The results of the total antioxidant capacity, reducing power and scavenging activity of DPPH, hydrogen peroxide and hydroxyl radical for all five fractions from EBL have been represented in **Table 5.4**. The total antioxidant capacity was determined by linear regression equation and was expressed as number of equivalents of ascorbic acid. Total Antioxidant capacity of EAF was found to be 92.46 ± 1.91 µg/ml which was higher as compared to other fractions. Assay of reducing power is a concentration dependent reaction i.e., higher concentration indicates higher reducing power. The results demonstrated a potent reducing potential of EAF (4.08 ±0.44 µg/ml) among all the fractions. The capability to reduce DPPH by donating an electron or hydrogen to DPPH is indicative of free radical scavenging activity of the phyotoconstituents. EAF showed an IC_{50} value of 61.00 ±1.60 µg/ml. Griess reagent was used to determine the

nitric oxide scavenging activity, which illustrated a good scavenging activity of EAF (IC_{50}: 48.52 ±3.64 µg/ml) but moderate scavenging activity of other fractions in comparison to rutin (IC_{50}: 31.92 ±1.84 µg/ml). A considerably good scavenging potential of hydrogen peroxide by EAF (IC_{50}: 27.23 ±1.31 µg/ml) was observed as compared to standard rutin (IC_{50}: 15.29 ±0.86 µg/ml) Fenton reaction was used to assess the potential of EAF in inhibiting the hydroxyl radical production through iron (II)–dependent deoxyribose damage assay. The results showed significant scavenging activity with an IC_{50} value of 42.37 ±1.84 µg/ml compared to positive control BHA (IC_{50}: 31.73 ± 1.91 µg/ml).

Table 5. 4- *In vitro* antioxidant activities of fractions from EBL

	IC_{50} ±SEM(µg/ml)**			
Drug	**DPPH radical**	**Nitric Oxide**	**H_2O_2 radical**	**Deoxyribose**
Standard	Ascorbic acid	Rutin	Rutin	BHA
	46.58 ± 1.95*	31.60 ± 1.84*	14.21 ± 0.86*	31.63 ± 1.91*
Sample				
Hexane fraction (HF)	113.61 ± 4.93*	67.55 ± 7.21	53.37 ± 5.21	79.36 ± 2.49
Ethyl Acetate fraction (EAF)	57.92 ± 3.40*	49.87 ± 3.64*	27.45 ± 1.31*	41.46 ± 1.84*
Dichloromethane fraction (DCMF)	69.34 ± 6.67	74.92 ± 4.95	37.34 ± 2.63*	50.83 ± 3.18
Butanol fraction (BuOHF)	93.32 ± 3.52	70.41 ± 7.92	51.72 ± 2.59	61.69 ± 2.48
Aquous fraction (AF)	121.89 ± 6.08	89.25 ± 5.44	59.45 ± 3.74	85.91 ± 4.54

**The results are average of three determinations ± SEM.

* Statistically significant as compared to positive control ($p<0.05$).

5.2.3 *In vitro* anti-inflammatory activity of fractions from EBL

5.2.3.1 Inhibition of albumin denaturation

Loss of structure and function of a protein because of damage caused by physical, chemical, or biological means is called protein denaturation. Hence, tissue protein denaturation serves as indicator of inflammation. In current study, the *in vitro* anti-inflammatory potential of PLSNPs and the fractions was assessed through inhibition protein denaturation. As set forth in **Table 5.5**, EAF demonstrated the highest potential in preventing the albumin denaturation, with IC_{50} value of 93.65 µg/ml. The results are comparable with that of the standard drug aspirin.

Table 5. 5- I*n vitro* Anti-inflammatory activity fractions from EBL

	IC_{50} ±SEM*(µg/ml)	
Drug	**Albumin denaturation**	**Anti-proteinase activity**
Aspirin	50.56±4.01*	46.61±2.80*
Hexane fraction (HF)	122.74 ± 4.48	141.53 ± 6.94
Ethyl Acetate fraction (EAF)	93.97±5.64*	96.41±7.20*
Dichloromethane fraction (DCMF)	109.37±6.31	138.62±5.79
Butanol fraction (BuOHF)	134.86 ± 5.73	127.19 ± 6.42
Aquous fraction (AF)	116.59 ± 4.56	125.32 ± 5.68

*The results are average of three determinations ± SEM.

* Statistically significant as compared to positive control ($p<0.05$).

5.2.3.2 Antiproteinase activity

Inflammatory reactions involve various agents such as proteinases. For example, leukocyte proteinases have significant role in tissue damage caused in inflammatory reactions. Hence, inhibition of these proteinases can help in protection of tissue damage. As given in **Table 5.5**, EAF demonstrated highest efficacy in preventing the proteinases, with IC_{50} value of 94.99 µg/ml. The results are comparable with that of the standard drug aspirin.

5.2.4 Standardization of fractions from EBL and quantification of phytoconstituents by HPTLC

The HPTLC fingerprint of EBL fractions (AF, EAF, HF, BuOHF, DCMF) for qualitative analysis are represented in **Figure 5.2A**. The fingerprinting analysis revealed the presence of various compounds especially terpenoids and steroidal constituents. EAF showed a greater number of spots with high area of peaks indicating a greater number of constituents being isolated as compared to other fractions. The amount of campesterol, lupeol, quercetin and rutin in the bands were estimated in EAF from the linear regression equation ($y= 8.89 \times 10^{-9}x$, $y= 3.67 \times 10^{-9}x$, $y= 8.02 \times 10^{-9}x$, $y= 3.37 \times 10^{-9}x$, respectively) obtained from amount per spot v/s respective area. Campesterol, lupeol, quercetin and rutin was quantified in EAF and was found to be 301.850±0.02 mg/g, 267.493±0.37 mg/g, 118.850±0.28 mg/g and 64.21±0.67 mg/g respectively **(Figure 5.2B-D).**

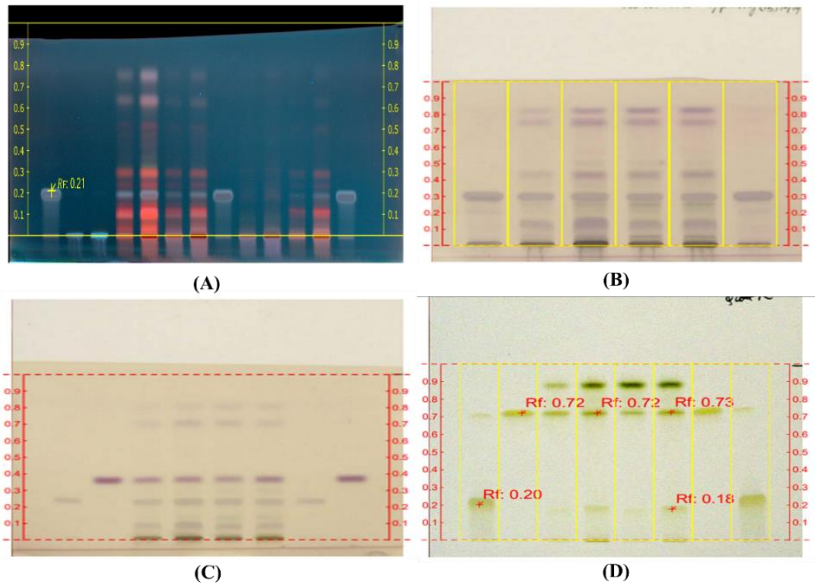

Figure 5. 2: A) HPTLC fingerprinting analysis of all five fractions of EBL B) Quantification of campesterol in EBL and EAF C) Quantification of lupeol in EBL and EAF D) Quantification of quercetin (Rf 0.72) and rutin (Rf 0.20) in EBL and EAF.

5.2.5 Standardization of EAF by HPLC

Using HPLC technique, campesterol was quantified in EAF. The amount of campesterol was found to be 218.678±0.52 mg/g in EAF **(Figure 5.3 A-B).**

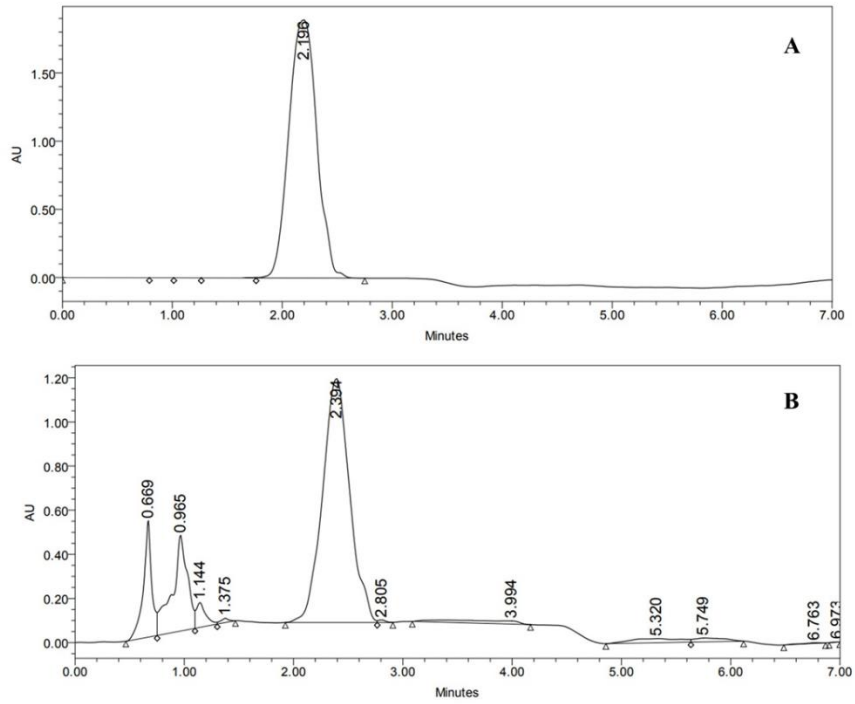

Figure 5. 3: HPLC chromatogram of A) standard campesterol and B) EAF

5.2.6 Molecular docking studies on Endothelin 1 and cytokines (TNFα and IL-6)

5.2.6.1 Molecular docking studies on Endothelin 1

The compounds from EAF showed binding energies between -769 to -10.42 Kcal/mol on endothelin 1 protein **(Table 5.6)**. Among all tested ligands lupeol exhibited significant binding energy (-10.42 Kcal/mol) compared to reference compound K-8794. The compound lupeol formed interactions with active site residues of endothelin 1 as follows Cys255 (H bond), His150 (pi-sigma and pi-alkyl), Ala154 (alkyl), Ile155 (alkyl), Val177 (alkyl), His167 (pi-alkyl), Phe240 (pi-alkyl), and Trp336 (pi-alkyl) **(Figure 5.4A & 5.4B).** The molecular docking results suggest lupeol is a well-suited moiety and was well resided active site of endothelin 1.

5.2.6.2 Molecular docking studies on AMPK

The isolated compounds from fraction name showed binding energies between -5.19 to -7.04 Kcal/mol on AMPK protein **(Table 5.6)**. Among all tested ligands, lupeol exhibited significant binding energy (-7.04 Kcal/mol) compared to reference compound (3-[4-(2-hydroxyphenyl) phenyl]-4-oxidanyl-6-oxidanylidene-7H-thieno[2,3-b] pyridine-5-carbonitrile). The compound lupeol formed interactions with active site residues of AMPK as follows Lys29 (alkyl), Ile46 (alkyl), Lys51 (alkyl), Val11 (alkyl), Leu18 (alkyl), Lys31 (alkyl), and Phe90 (pi-alkyl) **(Figure 5.4C & 5.4D).** The molecular docking results suggest lupeol is a well-suited moiety and was well resided active site of AMPK.

5.2.6.3 Molecular docking studies on Interleukin 6

The screened moieties displayed binding energies of -3.40 to -6.52 Kcal/mol and campesterol exhibited significant binding energy (-6.52 Kcal/mol) compared to other tested ligands **(Table 5.6).** Further compound campesterol showed strong binding profile at active site of IL 6, the observed interactions are Arg179 (H bond), Arg182 (H bond), and Tla300 (H bond) **(Figure 5.4E & 5.4F).** The compound campesterol binding mode and interaction profile were comparable to reference compound tartaric acid, it indicates campesterol can be used as an IL6 modulator.

5.2.6.4 Molecular docking studies on TNFα

The compound lupeol was found to be more effective lead as compared to other compounds from EAF. The compounds displayed optimal binding energies between -2.67 to -6.44 Kcal/mol, and lupeol showed -6.44 Kcal/mol **(Table 5.6).** Further, mode of interaction profile of lupeol at TNFα active site was evaluated and observed amino acids are Leu57 (alkyl),

Val123 (alkyl), Tyr59 (pi-alkyl), and Tyr119 (pi-alkyl) **(Figure 5.4G & 5.4H).** The binding interactions and binding mode analysis suggest compound lupeol has well resided at active site of TNFα.

Table 5. 6- Molecular docking studies of reported compounds from EAF on Endothelin 1, AMPK, IL6, and TNFα.

Ligands	**Endothelin 1**		**AMPK**		**IL6**		**TNFα**	
	Binding energy (Kcal/mol)	Ligand efficiency	Binding energy (Kcal/mol)	Ligand efficiency	Binding energy (Kcal/mol)	Ligand efficiency	Binding energy (Kcal/mol)	Ligand efficiency
Campesterol	-9.18	-0.32	-6.39	-0.22	-6.24	-0.22	-5.20	-0.18
Lupeol	-10.42	-0.34	-7.04	-0.23	-5.48	-0.18	-6.44	-0.21
Sitogluside	-7.69	-0.19	-5.19	-0.13	-3.40	-0.08	-2.67	-0.07
Stigmasterol	-9.41	-0.31	-6.57	-0.22	-5.42	-0.18	-5.92	-0.20
K-8794	-10.71	-0.22	-	-	-	-	-	-
3-[4-(2-hydroxyphenyl)phenyl]-4-oxidanyl-6-oxidanylidene-7H-thieno[2,3-b]pyridine-5-carbonitrile	-	-	-5.94	-0.23	-	-	-	-
Tartaric acid	-	-	-	-	-3.92	-0.39	-	-
6,7-dimethyl-3-[(methyl{2-[methyl({1-[3-(trifluoromethyl)phenyl]-1h-indol-3-yl}methyl)amino]ethyl}amino)methyl]-4h-chromen-4-one	-	-	-	-	-	-	-2.68	-0.07

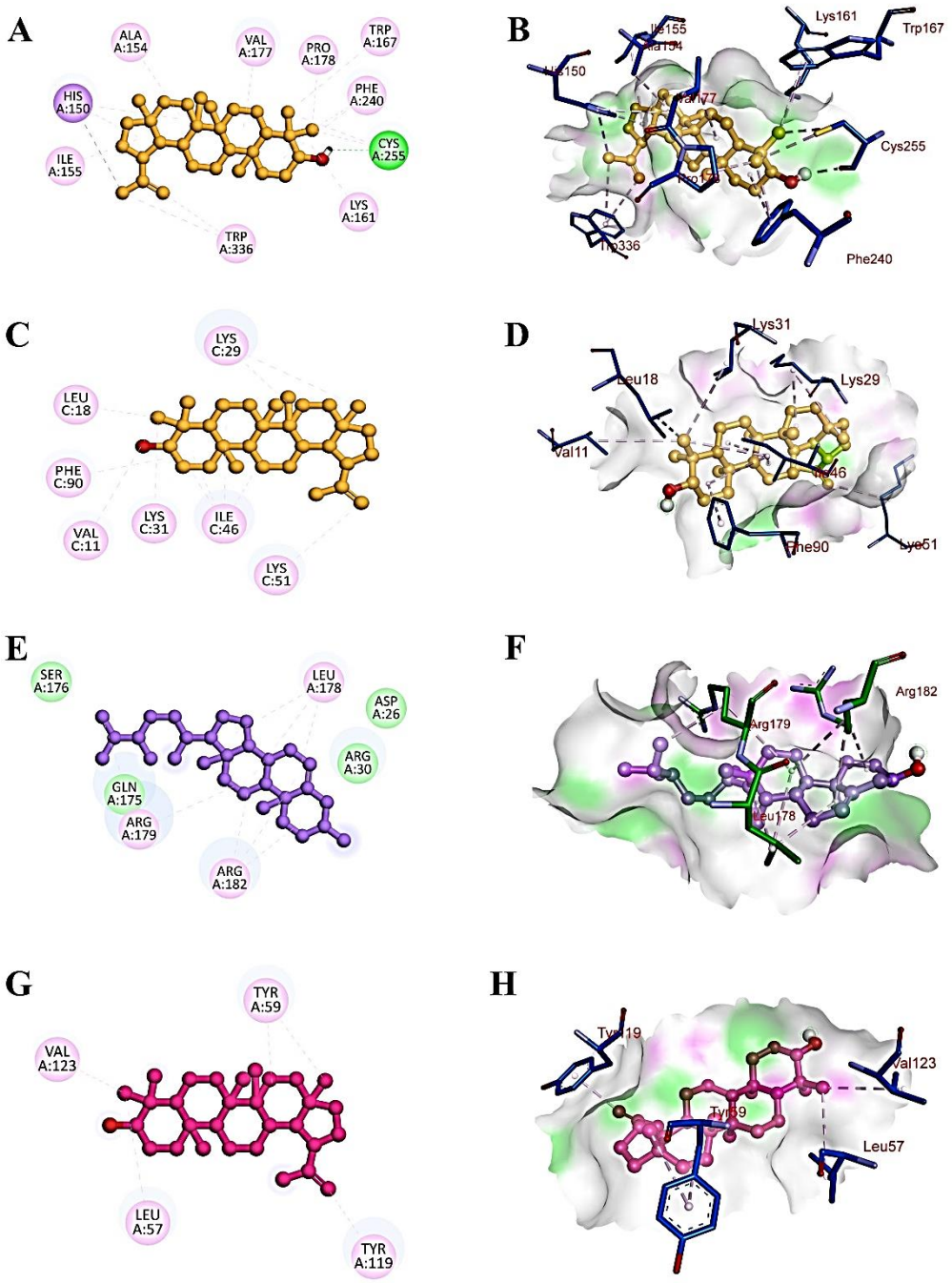

Figure 5. 4: (A) and (B) shows interaction of lupeol with amino acids at active site of ET_B protein (C) and (D) shows lupeol interaction with amino acids at active site of AMPK protein, (E) and (F) depicts campesterol interaction with amino acids at active site of interleukin 6, (G) and (H) shows lupeol interaction with amino acids at active site of TNFα protein.

5.2.7 Synthesis and confirmation of PLSNPs

In the current work, an attempt has been made to perform green synthesis of PLSNPs involving EAF obtained from EBL. The colour change from buff yellow to reddish brown within 24 hour was indicative of PLSNPs synthesis **(Figure 5.5-inset)**. Green synthesized PLSNPs were then examined and primarily confirmed using UV-Visible spectrophotometry. Upon analysis, the green synthesized PLSNPs showed absorption maximum (λ_{max}) at 410 nm while $AgNO_3$ solution had no such peak in visible range, as shown in **Figure 5.5**.

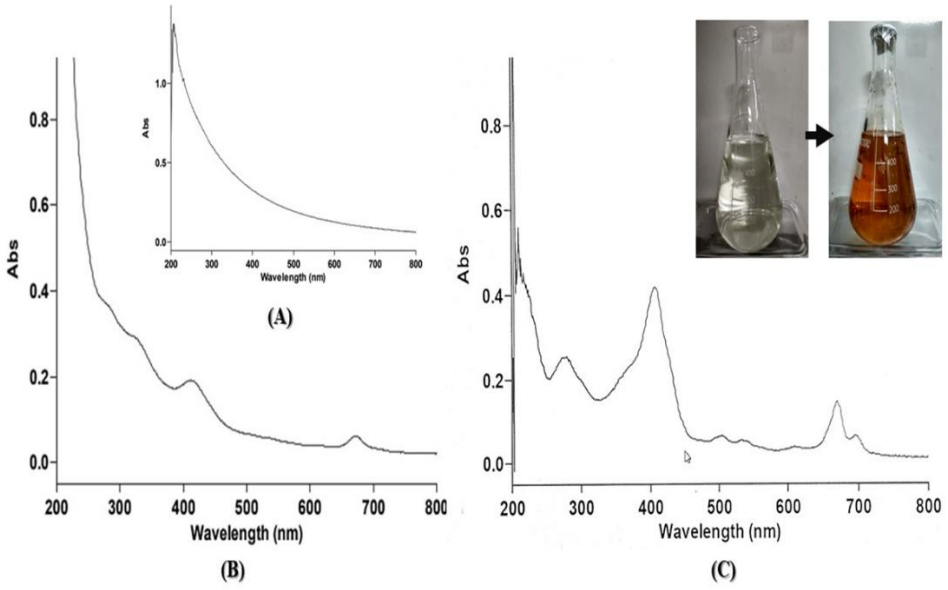

Figure 5. 5: UV spectra showing surface plasmon resonance at 410nm; A) Blank, B) start of reaction C) after 24 hours.

5.2.8 Process optimization

With the use of EAF derived from EBL, green synthesis of PLSNPs has been attempted in the current work. The process was optimized using BBD to obtain the nanoparticles of optimum size and to increase the entrapment efficiency to maximum level. Best response model was obtained by varying three astute factors viz. concentration of EAF, concentration of $AgNO_3$

and reaction time based on which optimized extraction cycle and condition was predicted. The final quadratic equations produced by the software with coded variables were as follows:

Particle size = 89.97375 + 12.38875*A + -12.895*B + 12.63125*C + -18.475*AB + -15.2175*AC + -15.39*BC + 6.879375*A^2 + -18.923125*B^2 + -15.650625*C^2 Eq (5.8)

Entrapment efficiency = 86.2025 + 17.04375*A + -0.49*B + 12.55875*C + -6.3125*AB + 7.35*AC + 7.3225*BC + -22.69625*A^2 + -7.61875*B^2 + -7.72625*C^2 Eq (5.9)

Selection of response model from amongst linear, 2FI, quadratic and cubic models to delineate obtained and expected outcomes, fitting of the data for observed responses to selected models and determination of significant factors are explained using **Table 5.7** and would not be expanded textually for the sake of preventing digression. Very briefly, though, quadratic model was selected to extract relationship amongst independent and dependent variables. The values of the coefficient for EAF and $AgNO_3$ concentration and reaction time, as given in equations, relates to effects of these factors and their comparative significance on the particle size and entrapment efficiency.

For instance, when the low concentration of $AgNO_3$ (2 mM) with relatively less amount of EAF (1 mg/mL) in Batch 11 was used, the entrapment efficiency was 35.67 % and the particle size was 60.19 nm. Whereas in Batch 14 when relatively higher concentration of $AgNO_3$ (4 mM) and EAF (2 mg/mL) was used there was a substantial increment in entrapment efficiency (99.7 %) and particle size (128.09 nm). The 3D response surface plots **(Figure 5.6A-D)** of DoE for extraction efficiency and phenolic yield suggested the following outcomes. The particle size and entrapment efficiency increased with increase in concentration of $AgNO_3$ and

EAF. The time of reaction also influenced the above outcomes as higher particle size with comparatively high entrapment efficiency was observed with increase in reaction time.

Table 5. 7- Model summary statistics and selection of significant factors

Entrapment Efficiency							Particle Size						
Model Selection	**Std. Dev.**	**R^2**	**Adj. R^2**	**Pred. R^2**	**PRESS**	**Remark**	**Model Selection**	**Std. Dev.**	**R^2**	**Adj. R^2**	**Pred. R^2**	**PRESS**	**Remark**
Linear	0.049	0.074	0.264	0.034	0.049		Linear	8.03	0.08	-0.09	-0.39	1564.16	
2FI	0.700	0.044	0.186	-0.525	0.697		2FI	8.55	0.15	-0.24	-1.12	2378.67	
Quadratic	0.006	0.533	0.685	0.162	0.0055	**Selected**	Quadratic	2.50	0.94	0.8941	0.48	575.86	**Selected**
Cubic	0.5329		0.6645		0.5329	**Aliased**	Cubic	1.96	0.98	0.9351		+	**Aliased**
	S.S.	**df**	**M.S.**	**F-value**	**p-value**			**S.S.**	**df**	**M.S.**	**F-value**	**p-value**	
Model	7866.72	9	874.08	5.59	0.0064	**Significant**	Model	10288.48	9	1143.16	5.17	0.0085	**Significant**
A	2323.92	1	2323.92	14.86	0.0032		A	1227.85	1	1227.85	5.55	0.0402	
B	1.92	1	1.92	0.0123	0.9140		B	1330.25	1	1330.25	6.02	0.0341	
C	1261.78	1	1261.78	8.07	0.0175		C	1276.39	1	1276.39	5.77	0.0371	
AB	159.39	1	159.39	1.02	0.3366		AB	1365.30	1	1365.30	6.18	0.0322	
AC	216.09	1	216.09	1.38	0.2671		AC	926.29	1	926.29	4.19	0.0678	
BC	214.48	1	214.48	1.37	0.2688		BC	947.41	1	947.41	4.29	0.0653	
A^2	2354.83	1	2354.83	15.05	0.0031	**Significant**	A^2	216.35	1	216.35	0.9788	0.3458	**Significant**
B^2	265.35	1	265.35	1.70	0.2220	**Significant**	B^2	1636.96	1	1636.96	7.41	0.0215	**Significant**
C^2	272.89	1	272.89	1.74	0.2160	**Significant**	C^2	1119.74	1	1119.74	5.07	0.0481	**Significant**
Residual	1564.32	10	156.43				Residual	2210.39	10	221.04			
Lack of Fit	398.74	3	132.91	0.7982	0.5329	**Not significant**	*Lack of Fit*	0.7637	3	0.2546	0.0008	1.0000	**Not significant**
Pure Error	1165.58	7	166.51				*Pure Error*	2209.62	7	315.66			
Cor Total	9431.04	19					Cor Total	12498.86	19				

Footnote: Std. Dev.: Standard deviation of obtained values over 15 runs; R^2: Regression coefficient (the model maximizing R^2 is selected); Adj. R^2: Adjusted R^2; Pred. R^2: Predicted R^2 (The selected model should maximize summation of Adj. R^2 and Pred. R^2); PRESS: Predicted residual sum of squares (PRESS statistic with the lowest value indicates the best model); 2FI:2 Factor Interaction Model;+: PRESS statistic can't be estimated; Aliased(Implies the number of experimental runs is not adequate to fit cubic model in the response curve); S.S.: Sum of Squares; M.S.: Mean Square; df :Degree(s) of freedom. After adapting quadratic model, influence of each factor (A, B, C...C^2) was verified by computing F values. Factor with large F value explains the variance more. Probability of obtaining this F value, if the investigated independent variable did not have any effect on the response is measured by p values. Small probabilities, $p<0.05$, indicate a significant factor. The insignificant lack of fit for the quadratic model counter intuitively proves that the model is a good fit and can be pursued for optimization of nanoparticle (PLSNPs) synthesis.

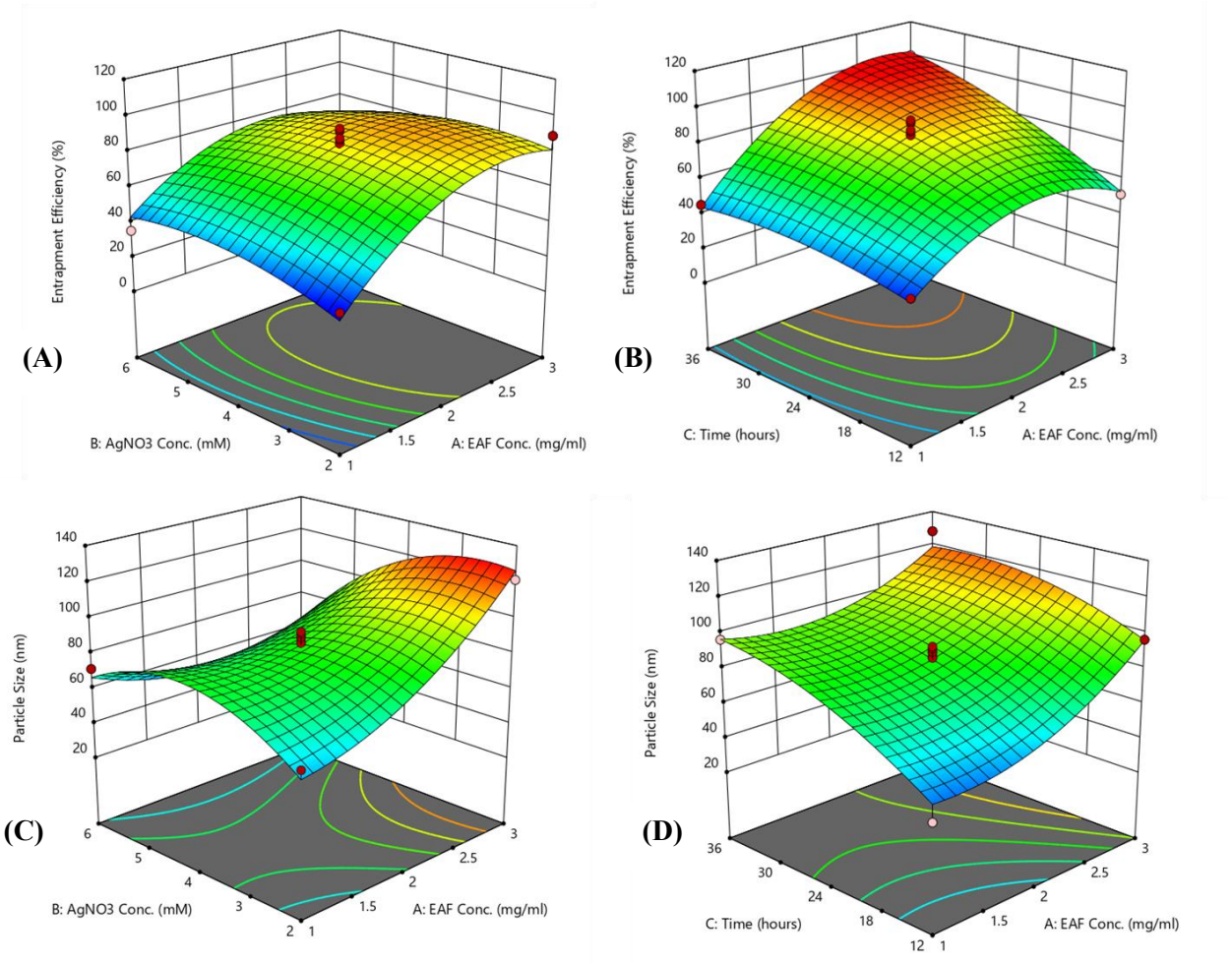

Figure 5. 6: 3D- response surface plots by Design Expert explaining the biosynthetic process. (A) and (B) represent the effect of time, EAF conc. and $AgNO_3$ conc. on entrapment efficiency; (C) and (D) represent the effect of time, EAF conc. and $AgNO_3$ conc. on particle size.

5.2.9 Checkpoint analysis (validation of method)

The predicted values of Y1 and Y2 were 84.784 nm ($n = 3$) and 97.444 %, respectively and the actual experimental values of Y1 and Y2 were 83.313±1.38 and 96.413±1.46. The percentage prediction error (% Bias) for the checkpoint batch was found to be − 1.738% and -1.058% respectively, which was < ±5% validating the authenticity of predictive capacity and accuracy of the design model.

5.2.10 Characterization of PLSNPs

5.2.10.1 ATR-FTIR analysis

By using the ATR-FTIR approach, the operationally engaged groups in EAF that were in charge of reducing Ag+ to PLSNPs were analysed. Three major peaks around 3400 cm^{-1}, 2100 cm^{-1}, and 1740 cm^{-1} **(Figure 5.7)** corresponding to alcoholic or phenolic OH as well as CH and CO bonds due to vibrational stretching were observed in both EAF and PLSNPs. The recognisable peak at 1101 cm-1 due to vibrational stretching of CO bond was only evident in EAF but was absent in PLSNPs; this may be due to involvement this bond in the reduction of Ag^{+} to PLSNPs. Therefore, it is possible to infer from the FTIR spectra that the active constituents of EAF were the main agents behind conversion of Ag+ to PLSNPs. Additionally, the PLSNPs were coated with phytochemicals, which prevented them from aggregating.

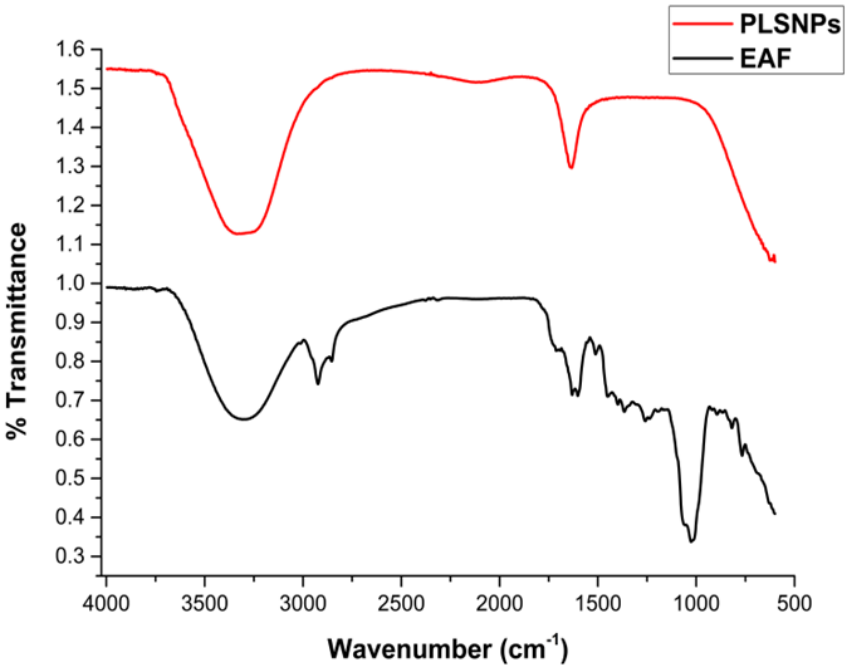

Figure 5. 7: ATR-FTIR spectra of silver nanoparticles PLSNPs (red) and EAF (black).

5.2.10.2 Morphological characterization

The average particle size of PLSNPs was determined by means of dynamic light scattering (DLS) instrument upon completion of the reaction. Bio-reduction of Ag^{+} ion to Ag^{0} yielded the PLSNPs with average particle size of 77.56 nm. The polydispersity index (PDI) of PLSNPs was recorded as 0.258, complying with monodispersive distribution system.

The size and shape of PLSNPs were assessed through TEM and SEM. TEM images were used to create a particle size distribution histogram, which revealed that the average particle size of PLSNPs was 85.64 nm, falling within the range of 20-120 nm observed in SEM with almost spherical shape **(Figure 5.8A-C)**. The large size particles observed, might be formed due to the aggregation of PLSNPs during the process of drying.

The histogram **(Figure 5.8C)**, which depicts the distribution of various particle sizes as determined by ImageJ software, revealed that the average particle size was in the range of 85.64 nm. The percentage of silver and carbon elements were found to be 87.41% and 12.59% respectively in the EDS analysis. The presence of carbon was indicative of the involvement of phytoconstituents in biosynthesis and capping of PLSNPs **(Figure 5.8D)**. The absence of oxygen in the EDS spectrum suggests that synthetic PLSNPs restrict oxidation.

In the XRD pattern of the PLSNPs, high intensity diffraction peaks at 2Θ angles of 38.50°, 44.94°, 64.50°, and 76.60° were observed (**Figure 5.8E**). The peaks, which correspond to the (1 1 1), (2 0 0), (2 2 0), and (3 1 1) reflections of the face-centered cubic (FCC) structure, were in agreement with those of the Joint Committee on Powder Diffraction Standards (JCPDS file No. 04-0783) [148, 149]. By observing the orientation towards the plate 111, crystalline nature of PLSNPs was confirmed. The peaks designated with an asterisk in the figure were observed

as a result of phytoconstituents crystallising on the surface of PLSNPs indicating the encapsulation. The results supplemented the SEM findings.

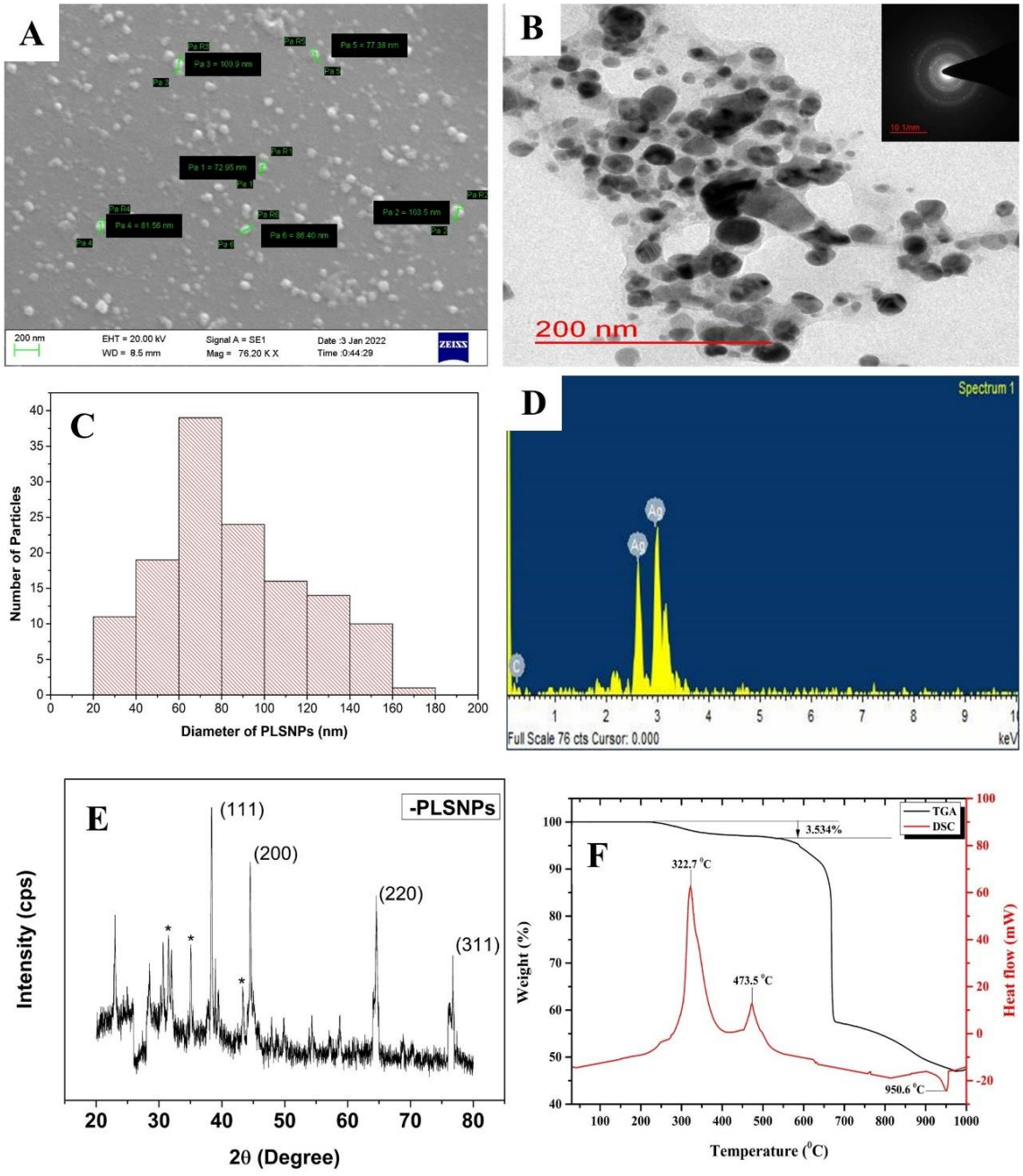

Figure 5. 8: Morphological and thermal analysis of PLSNPs through A) SEM showing shape and size, B) TEM and SAED (inset), C) distribution of different size PLSNPs, D) EDAX analysis, E) X-ray diffraction (XRD) F) TGA (black) & DSC (red).

5.2.10.3 TGA and DSC analysis

Under a nitrogen environment, the thermal behaviour of the produced PLSNPs has been examined using TGA and DSC techniques. PLSNPs exhibited thermal degradation in two phases between 200 to 800 °C. The first phase weight loss of 3.5% around 200°C showed the initial loss of phytoconstituents present at the outermost surface of PLSNPs, later, the PLSNPs were stable up till 600°C and a sudden change in weight was observed around 700°C indicating the loss of phytoconstituents conjugated strongly to the metal core **(Figure 5.8F)**. It has been computed that the solid mass remaining after weight loss is equal to the weight of metallic silver (43.0 % w/w). In DSC profile, two exothermic peaks had been noted at 322.7°C and 473.5°C. These exothermic peaks denoted the decomposition of organic layers in PLSNPs [8]. An endothermic peak around 900°C was also observed indicating the fusion of elemental silver.

5.2.11 Estimation of entrapment efficiency and drug loading capacity

The entrapment efficiency PLSNPs was found to be 86.85% while the loading capacity was found to be 53.474%.

5.2.12 *In vitro* release profile of PLSNPs

Release of campesterol from PLSNPs has been shown in **Figure 5.9**. The release pattern of campesterol was found to be rapid, as a liminal burst release was observed irrefutably in the first 4 hours in both the media. This release pattern could be expedient in ameliorating hemorrhoids by attaining the desired threshold of action rapidly. Almost 50% of release of campesterol in the first 4 hours was noted, with comparatively slower release rate afterwards.

An explication to this can be a rapid release of phytoconstituents capped on the outer surface followed by the release of phytoconstituents encapsulated in the core of PLSNPs [21, 24].

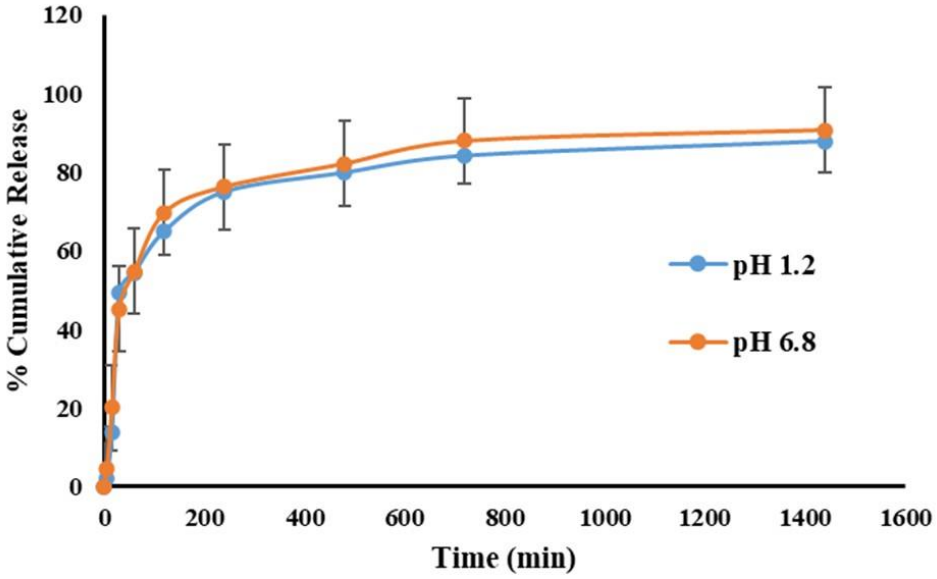

Figure 5. 9: *In vitro* drug release profile of campesterol from PLSNPs.

5.2.13 *In vitro* antioxidant activity

Total Antioxidant capacity of PLSNPs was found to be 82.78 ± 5.84 µg/ml. Results of reducing power assay demonstrated a potent reducing potential of PLSNPs (3.43 ±0.56 µg/ml) while PLSNPs showed an IC_{50} value of 75.53 ±3.40 µg/ml in DPPH assay as compared to ascorbic acid (IC_{50}: 46.58±1.94 µg/ml). The nitric oxide scavenging activity results indicated moderate scavenging activity of PLSNPs (IC_{50}: 53.39 ±3.09µg/ml) in comparison to rutin (IC_{50}: 31.92 ±1.84 µg/ml). A considerably moderate scavenging potential of hydrogen peroxide by PLSNPs was observed with an IC_{50} value of 32.68 ±1.93 µg/mL compared to standard rutin (IC_{50}: 15.29 ±0.86 µg/ml). Fenton reaction was used to assess the potential of PLSNPs in inhibiting the hydroxyl radical production through iron (II)–dependent deoxyribose damage assay. The

results showed significant scavenging activity with an IC_{50} value of 57.80 ±2.27 µg/ml compared to positive control BHA (IC_{50}: 31.73 ± 1.91 µg/ml).

5.2.14 *In vitro* anti-inflammatory activity of PLSNPs

In current study, the *in vitro* anti-inflammatory potential of PLSNPs and the fractions was assessed through inhibition protein denaturation. As per the results, PLSNPs demonstrated the significant potential in preventing the albumin denaturation (IC_{50}: 63.29 µg/ml) and antiproteinase activity (IC_{50}: 69.56 µg/ml). The results are comparable with that of the standard drug aspirin.

5.2.15 Antibacterial activity

The antibacterial efficacy of PLSNPs and EAF along with positive (gentamicin) and negative control (distilled water) were tested against respective Gram-positive (*S. aureus*) and Gram-negative (*E. coli*) pathogens using the agar well diffusion method and the results were presented in **Figure 5.10**. The zone of inhibitions on all pathogens was carefully measured after incubation of 24 h at 37°C. The result revealed that the PLSNPs exhibited higher antibacterial activity in terms of zone of inhibition against *E. coli* and *S. aureus* pathogens when compared to the EAF. The maximum zone of inhibition against *E. coli* (18.3 ± 2.08 mm for 50 µg/ml) and *S. aureus* (25.0 ± 1.19 for 50 µg/ml) was observed in PLSNPs treated wells. The EAF and antibiotic also displayed the antibacterial activity of 15.0 ± 1.4 mm and 30.4 ± 1.39 mm against *E. coli* whereas 20.7 ± 1.21 mm and 33.1 ± 1.90 mm against *S. aureus*, respectively. The minimum inhibitory concentration (MIC) study using the micro broth dilution method revealed that the MIC of PLSNPs against *E. coli* was found to be 30–80 µg/ml followed by EAF (50–80 µg/ml) and gentamicin (10–80 µg/ml) **(Table 5.8)**. For *S. aureus* the

MIC values were 20–80 µg/ml, 60–80 µg/ml and 10–80 µg/ml for PLSNPs, EAF and gentamicin respectively **(Table 5.8).**

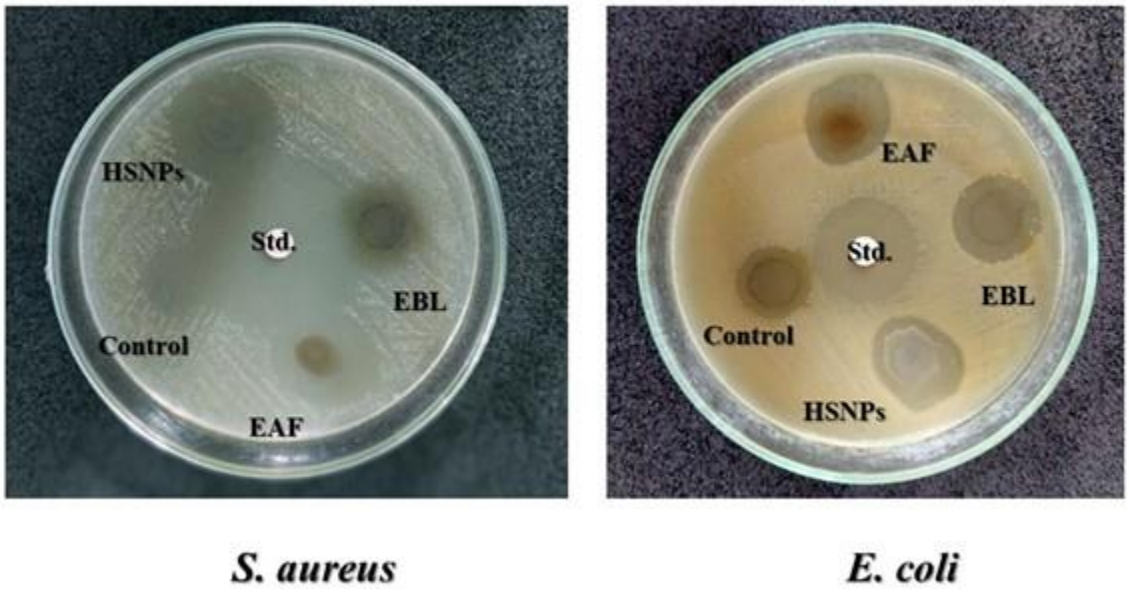

Figure 5. 10: Antibacterial activity of PLSNPs.

Table 5. 8- MIC value of PLSNPs, EAF and Gentamicin against *E. coli and S. aureus*

Drug		MIC*							
		Concentration (µg/ml)							
		10	20	30	40	50	60	70	80
Gentamicin	*E. coli*	+	+	+	+	+	+	+	+
	S. aureus	+	+	+	+	+	+	+	+
EAF	*E. coli*	-	-	-	-	+	+	+	+
	S. aureus	-	-	-	-	-	+	+	+
PLSNPs	*E. coli*	-	-	+	+	+	+	+	+
	S. aureus	-	+	+	+	+	+	+	+

***The results are average of three determinations ± SEM**

5.3 Discussion

Nanoscale based formulations has attracted the scientists worldwide because of its wide range of applicability, lesser toxicity and more palatability [150]. Biogenic and bio-fabricated nanoparticles involve one step-one pot process for their synthesis. This method of nanoparticles synthesis is cheaper, less hazardous, and less tedious.

As per previous reports, *Blumea lacera* is claimed to possess antioxidant, antibacterial, anti-inflammatory and anti-hemorrhoid activity [30]. Since, there is no scientific reports for the synthesis of bio-fabricated silver nanoparticles involving *Blumea lacera* and its medical applicability. Hence, to best of our knowledge we, for the first-time report synthesis, characterization, and evaluation of biological potency of silver nanoparticles (PLSNPs) using ethyl acetate fraction (EAF) from EBL in this study.

Polyphenol enriched plants are generally preferred for biogenic nanoparticles synthesis as high number of flavonoids and sterols could yield greater amount of PLSNPs [151-153]. Therefore, all the five fractions of EBL (hexane- HF, dichloromethane- DCM, ethyl acetate- EAF, butenol- BuOHF & Aquous- AF fractions) were quantified for total phenolics, flavonoids and flavanols and phytosterols through standard chemical methods chemical methods. The results suggested that ethyl acetate fraction (EAF) possessed highest content of total phenolics, flavonoids as well as flavanols and phytosterols.

Overproduction of reactive oxygen species (ROS) can alter the anatomy and physiology of various vital organs by damaging the DNA, proteins, tissues and neurotransmitter signalling pathways [122]. The role ROS in aetiology of various diseases have been established by many researchers [154, 155]. Drugs with natural origin possess high antioxidant capacity, therefore,

the all the fractions from EBL have been evaluated for their antioxidant potential in this study. The results showed that the EAF demonstrated significant anti-oxidant potential.

Inflammatory response to any kind external stimuli that causes alteration to normal anatomy and physiology of human tissue is the natural defence mechanism of human physiological system. This inflammatory response is very complex that involves several factors which may be associated with several diseases. However, use of steroidal and nonsteroidal anti-inflammatory drugs (NSAIDs) for the treatment of inflammation is common but use of these drugs causes serious side effects [135, 156]. Hence, in search of a better natural anti-inflammatory drug with lesser adverse events, all the fractions from EBL have been evaluated in this study and the results demonstrated high efficacy of EAF as anti-inflammatory agent than other fractions.

HPTLC and HPLC techniques give a thorough insight about the chemical nature of any natural material and are sophisticated tool for developing the standardized phytopharmaceuticals. In this study the HPTLC technique was exploited to quantify four different phytoconstituents i.e., campesterol, lupeol, quercetin and rutin in EAF derived from EBL. The results revealed that the EAF possessed a substantial amount (301.850±0.02 mg/g, 267.493±0.37 mg/g, 118.850±0.28 mg/g and 64.21±0.67 mg/g respectively) of these phytoconstituents. It should be noted that EAF possessed comparatively high content of phytosterols than flavonoids as evident from both the results of chemical quantification and HPTLC study. Therefore, EAF was further standardized for phytosterols (218.678±0.52 mg/g in EAF) using campesterol as standard marker.

Molecular docking studies are useful for predicting basic biochemical processes by modelling the interactions between phytochemical compounds and specific proteins responsible for pathophysiological states. The characterization of a compound's behaviour when it binds to target macromolecules has great importance in the evaluation of new compounds. In the current study, interaction of the active constituents (campesterol, lupeol, stigmasterol, sitogluside) from EAF with endothelin B, AMPK, TNF-α and IL-6 receptor proteins have been evaluated where campesterol, lupeol and stigmasterol were found to be active on the binding sites of these receptors. Activation of endothelin receptor ET_B leads to vasodilation as demonstrated in several studies [157, 158], therefore, blockade of ET_B receptor could be useful in the management of bleeding piles as it will cause vasoconstriction, restricting the blood flow in the haemorrhoidal tissue. The results showed that lupeol interacts with active sites of ET_B receptors in similar fashion as K-8794 (selective antagonist of ET_B receptor). To understand the mechanism by which low level of cytokines (TNF-α and IL-6) are exhibited in the treated animals, the interaction of phytosterols from EAF with AMPK was done. The results suggested that lupeol is a well-suited moiety and was well resided active site of AMPK. As per reports, activation of AMPK receptors leads to reduced cytokine levels via several molecular pathways [159]. Apart from inhibiting the release of the cytokines, the active constituents from EAF could also inhibit binding of these cytokines to their receptors by as shown in *in silico* study results leading to significant anti-inflammatory effect.

Formation of PLSNPs was confirmed by observing the characteristic peak at 410 nm in the spectra using UV-Visible absorption spectroscopy: a prominent analytical tool for measuring SPR and for investigation of the optical properties of PLSNPs. The peak at 410 nm shown by PLSNPs, in the current study, was within the range (400-480 nm) of the characteristic SPR

exhibited by silver nanoparticles [160]. The results of XRD revealed the pattern of PLSNPs suggestive of crystalline nature of the particles. The intense diffraction peaks at (111), (200), (220) and (311), for PLSNPs were in accordance with the Joint Committee on Powder Diffraction Standards (JCPDS) file no. 04-0783 for silver. For determining different functional groups FT-IR spectroscopy is applied. In the current study, FT-IR analysis was done to determine the plausible phytoconstituents from EAF which are primarily involved in reduction of $AgNO_3$ and formation of PLSNPs along with capping on its surface. The results of FTIR showed the presence of hydroxyl and carbonyl functional groups, indicating the presence of phytosterols and flavonoids in the stabilized PLSNPs [161]. As per reports, the carbonyl, hydroxyl and other functional groups present in phytoconstituents might be responsible for nanoparticle formation involving the mechanism of nucleation, complexation and dimerization [162, 163]. SEM and TEM characterization results demonstrated the smooth, uniform, monodispersed, spherical shape of PLSNPs. In the SAED pattern, polycrystalline nature of the PLSNPs were observed which were compliant to the XRD results and earlier studies [164, 165]. The average particle size of PLSNPs was found to be ~86 nm from the particle size distribution histogram. Although, minimal agglomeration has been observed indicating the presence of phytoconstituents on PLSNPs surface.

Drug loading capacity is defined as the ratio of the practically determined percentage of drug content as compared to theoretical mass of drug used in the formulation of the nanoparticles [166]. The drug loading capacity is dependent on the polymer-drug combination and the method applied. Hydrophobic polymers tend to encapsulate larger amounts of hydrophobic drug and vice-versa [166]. Several formulation factors, such as type of stabilizing agent and polymer-drug mass ratio will influence the extent of drug loading [167]. In biofabrication of

silver nanoparticles, this stabilization is achieved via capping of phytoconstituents on the surface of reduced metal[161]. In this study, the loading capacity was determined and was found to be (53.474%).

During drug development process it becomes necessary to determine the behavior and assure the quality of the drug to establish *in vitro in vivo* correlation (IVIVC), hence *in vitro* drug release kinetics becomes an important tool for assessing the aforementioned parameters [168]. In current investigation, the release pattern of campesterol from PLSNPs was observed which revealed that the release of campesterol was faster at first enabling it to acquire rapid onset of action but was slower at later stage extending, its mean residence time (MRD). This release behaviour of campesterol is supporting the claim of capping the PLSNPs.

Overproduction of reactive oxygen species (ROS) can alter the anatomy and physiology of various vital organs by damaging the DNA, proteins, tissues and neurotransmitter signalling pathways [122]. The role ROS in aetiology of various diseases have been established by many researchers [154, 155]. Drugs with natural origin possess high antioxidant capacity, therefore, the biogenic PLSNPs along with all the fractions from EBL have been evaluated for their antioxidant potential in this study. The results showed that the EAF demonstrated significant anti-oxidant potential as compared to other fractions, furthermore, PLSNPs displayed no significant antioxidant effect than that of EAF. One of the major reasons behind this may be the loss of polyphenols and sterols during the reduction of $AgNO_3$ for the formation PLSNPs.

Inflammatory response to any kind external stimuli that causes alteration to normal anatomy and physiology of human tissue is the natural defense mechanism of human physiological system. This inflammatory response is very complex that involves several factors which may

be associated with several diseases. However, use of steroidal and nonsteroidal anti-inflammatory drugs (NSAIDs) for the treatment of inflammation is common but use of these drugs causes serious side effects [135, 156]. Hence, in search of a better natural anti-inflammatory drug with lesser adverse events, the potential of PLSNPs as anti-inflammatory drugs have been evaluated. As evident from the results, PLSNPs possess high efficacy as anti-inflammatory agent than EAF and may be good alternative to combat the complications caused during inflammation. These anti-inflammatory property of PLSNPs may be due to the retainment of phytosterols on the surface of PLSNPs as these constituents have been studied rigorously as anti-inflammatory agents acting through several mechanisms such as phagocytosis, suppression of cytokines (TNF-α) production and also inflammatory mediators like COX-2 and iNOS [169, 170].

Search for new antibacterial to combat the resistance developed by microorganisms has been one of the major thrust areas of drug discovery. Nanoparticles being smaller in size with high surface area are a better alternate for conventional antibacterial agents. Moreover, the biogenic nanoparticles capped with phytoconstituents can act on microorganisms through several simultaneous mechanisms preventing the development of resistance by the microbes [171, 172]. The results of antibacterial assay showed that the PLSNPs have significant antibacterial activity against both types (G- & G+) of pathogens (*E. coli and S. aureus*) when compared to EAF, this may be attributed to spherical shape and smaller size of PLSNPs. The smaller size of PLSNPs enables it to react with sulphur and phosphorus groups of amino acids on the cell membrane which in turn alters the surveillance of bacteria and to penetrate the cell wall of bacteria [173, 174]. Furthermore, ionic silver from PLSNPs gets attached to negatively charged

particles on bacterial cell wall which leads to change in the cell wall composition ultimately affecting cell permeability [174].

5.4 Conclusion

The current study focused on the green synthesis of PLSNPs utilizing the EAF fraction prepared from ethanolic extract of *Blumea lacera* by "one step-one pot process". Molecular docking results revealed the interaction of phytoconstituents present in EAF with AMPK and ET_B receptors in similar fashion as standard anti-inflammatory drugs which may contribute to its antihaemorrhoidal potential. Upon characterization, the PLSNPs showed spherical shape with average particle size of 20-30 nm. Phytochemical analysis of the fraction revealed the presence of phenolic compounds, phytosterols, and flavonoids responsible for reduction and capping of PLSNPs. Later, the release pattern of campesterol from PLSNPs confirmed the above observation. From the results of antioxidant, anti-bacterial and *in-vitro* anti-inflammatory activity, it is evident that PLSNPs can be good alternative to the currently used medicines for treating bacterial infections and inflammation. Therefore, it can be concluded that biological synthesis of PLSNPs using EAF from EBL is efficient and economical process and PLSNPs synthesized through this process can be potential agents in amelioration of various inflammation related pathological conditions. Although, more rigorous *in-vivo* studies need to be conducted in future to get deep insight of the actual mechanism taking place behind these pharmacological activities.